JEE Journal of Ecological Engineering

Journal of Ecological Engineering 2023, 24(9), 282–292
https://doi.org/10.12911/22998993/169289
ISSN 2299–8993, License CC-BY 4.0

Received: 2023.05.19
Accepted: 2023.07.06
Published: 2023.07.24

Characteristics of Silica Powder Extracted from Fly Ash of Coal Fired Power Plant – Effect of Heat Treatment Process

Nurmalita Nurmalita[1,3], Syahrun Nur Abdulmadjid[2], Adi Setiawan[3], Rinaldi Idroes[4], Zulkarnain Jalil[2*]

[1] Graduate School of Mathematics and Applied Sciences, Syiah Kuala University, Darussalam, Banda Aceh 23111, Indonesia

[2] Department of Physics, Faculty of Mathematics and Natural Sciences, Syiah Kuala University, Darussalam, Banda Aceh 23111, Indonesia

[3] Department of Mechanical Engineering, Faculty of Engineering, Malikussaleh University, jalan Batam, Bukit Indah, Lhokseumawe 24351, Indonesia

[4] Department of Chemistry, Faculty of Mathematics and Natural Sciences, Syiah Kuala University, Darussalam, Banda Aceh 23111, Indonesia

* Corresponding author's email: zjalil@unsyiah.ac.id

ABSTRACT

Fly ash waste is a by-product of coal burning at PLTU Nagan Raya, Aceh Province, Indonesia. Since 2017, the coal used is a mixture of 90% Kalimantan coal (sub-bituminous) and 10% local Nagan Raya coal (lignite) which is still young so that the mineral ash content is still high. Silica is among the interesting minerals to be extracted from fly ash, given its wide range of benefits. This paper describes the process of extracting silica from fly ash at the Aceh power plant through the leaching method using a chemical solution and heating for 2 and 4 hours at a temperature of 100˚C. The difference in heat treatment aimed to study the changes in properties and obtain the best method in the silica extraction process. The effect of heat treatment on silica characteristics was studied based on X Ray Diffraction (XRD) test for phase identification, Scanning Electron Microscopy (SEM) test for morphological identification, Energy Dispersive X-Ray Spectroscopy (EDS) test for mineralogy element identification, Fourier Transform Infra-Red (FTIR) test for identification of functional groups and surface chemistry, and differential calorimetric analysis/ thermogravimetric (DSC/TGA) test for identification of thermal properties. As a result, it was found that fly ash still contains unburned carbon, which significantly affects its color, and has the potential for application as a hydrogen storage material because its pore diameter structure is larger than 0.7 nm. The silica extracted from fly ash is capable of achieving a purity of up to 87% and exhibits excellent thermal stability, especially at temperatures between 120–300 °C; thus, it has the potential to be a catalyst material in the adsorption-desorption reaction of hydrogen by magnesium, although further research is still needed.

Keywords: fly ash; coal; power plant; pyrolysis; heat treatment; surface area; adsorption.

INTRODUCTION

Coal is an important fuel in the operation of steam power plants (PLTU). Coal is burned to boil the water in the boiler to produce steam that can drive turbines to generate electricity. Coal burning produces waste in the form of coal ash, coal gasification ash, coal bottom ash, and fly ash (Juda-Rezler and Kowalczyk, 2013). Coal fly ash is waste from burning coal in power plants spread across the globe, supplying 47% of the global electricity needs by 2030 (Yao et al., 2015)(Muthusamy et al., 2020). One of the coal-fired power plants in Indonesia is the Nagan Raya Power Plant in Aceh Province, which has a capacity of 220 MW. On average, this power plant burns approximately 50 thousand tons of coal every month to supply 50% of the electricity required in Aceh. On the basis of statistical data, the level of fly ash from burning Indonesian coal ranges from 7.5%-10% (Petrus

et al., 2020). It is estimated that the Aceh power plant produces approximately 3750 tons of coal ash waste every month.

The characteristics of fly ash vary depending on the type, origin and degree of fragmentation of the coal used, the technology and temperature of combustion and storage method (Gruchot and Zydroń, 2016). Generally, coal fly ash is composed of silica (SiO_2), ferrous oxide (Fe_2O_3), alumina (Al_2O_3), calcium oxide (CaO), titanium oxide (TiO_2), magnesium oxide (MgO), alkaline (Na_2O and K_2O), sulfur trioxide (SO_3), phosphorus oxide (P_2O_5) and the residue is carbon dioxide on fire (Blissett, 2015). In general, the main composition is Al_2O_3, SiO_2 and Fe_2O_3 while the oxides of Mg, K, Ca, and Na were found in low concentrations (Lindvall et al., 2017).

The color of fly ash varies from gray to black depending on the amount of carbon content. The higher the carbon value content, the blacker the fly ash color (Yadav and Fulekar, 2020). The main minerals that form the crystalline phase in fly ash are quartz (SiO_2) and mullite ($3Al_2O_3•2SiO_2$) which are reactive only under conditions of high temperature and high pressure (Foo et al., 2019). The calcium in fly ash can form several phases, but generally CaO. However, CaO easily turns into gypsum and ettringite due to humid conditions after coal combustion (Vilakazi et al., 2022). Fly ash also contains an iron crystalline phase in the form of hematite (ÿ-Fe_2O_3), magnetite (Fe_3O_4), and maghemite (ÿ-Fe_2O_3) which are highly reactive to acid solutions (Fomenko et al., 2021; Handoko et al., 2020). Generally, the crystalline phase of fly ash is known quite clearly, while the amorphous phase has a very complex arrangement of elements (Song et al., 2020).

Fly ash has waterproof properties and is divided into two types, that is class F fly ash which is the result of burning anthracite coal (coal bituminous), and class C fly ash produced from lignite (bituminous sub coal) (Bhatt et al., 2019). Class C contains 70% of the mineral silica. This is because the mineral ash content is quite high from low-rank coal combustion (Wang et al., 2019). Pure crystalline silica has two stable forms i.e quartz and cristobalite (Monfort et al., 2014). Silica trydimite can also be found in fly ash formed at fairly high temperatures. Silica is relatively unreactive to H_2, Cl_2, acids and most metals at a temperature of 25°C or higher, but is soluble in phosphoric acid, hydrofluoric acid (HF), carbonate and alkaline hydroxide (Sefriani and Oktavia, 2021). In general, the extraction of silica from coal fly ash is carried out by the process acid washing (Guo et al., 2019).

The process of washing with an acid solution can increase the purity level of silica and reduce impurities that are usually metal oxides. Acid solution is used in the form of H_2SO_4 (Mohammed Hello and Kadhim Hlial, 2019) or HCl (Dhaneswara et al., 2020). The acid solution is able to reduce the aluminum content by 94.23% and reduce the iron content by 97.96% (Anas Boussaa et al., 2017). The use of sulfuric acid also removes zinc during the silica refining (Vielma et al., 2018). The use of alkaline NaOH solution during the purification process is useful for binding silica as sodium silicate under acidic conditions (Abu Bakar and Jia Ni Carey, 2020) and finally the process will be obtained silica powder with a certain purity.

The purpose of this study was to study the silica extraction process from coal ash waste at the Aceh power plant and examine the characteristics of silica and other potential mineral content. The extraction process uses HCl solution for initial washing to reduce the content of aluminum, iron and zinc. Silica characterization was carried out through BET (N_2 isothermal adsorption-desorption) analysis, XRD spectrum, FTIR spectrum, SEM/EDS, and DSC/TGA thermal analysis.

METHODOLOGY

Materials

The coal fly ash used in this study was collected from a steam power plant (PLTU), located in Nagan Raya, Aceh Province, Indonesia with a capacity of 220 MW. Fly ash is passed through a sieve of 200 mesh to obtain a uniform particle size. Hydrochloric acid (purity 38%, Merck) diluted to a concentration of 1 M, hydroxide sodium solution (Merck) 1M and aquadest are used in the extraction process as solvents.

Silica extraction

A total of 40 grams of coal fly ash was mixed with 100 ml of 1M HCl solution and heated in an oven at 90°C for 4 hours until a precipitate formed. Furthermore, the precipitate is filtered using filter paper and washed with aquadest until the pH of the washing water becomes neutral (the

pH of the washing water until it reaches about 7, means that the remaining HCl in the precipitate has disappeared) and the precipitate is dried in the oven for 12 hours at a temperature of 110°C. The dried precipitate is then dissolved with a 3M NaOH solution at a temperature of 90°C. The soaking process is varied with a time of two hours and four hours until it is completely submerged to dissolve the silica content and form a solution of sodium silicate. Then, a solution of HCl 1M which has been diluted with aquadest where the ratio is 1:1 is added. The diluted HCl solution is added little by little while stirring gently until a whitish precipitate form under acidic conditions and left for 18 hours. Then, the whitish-gray precipitate is filtered and washed several times with aquadest until the washing water is neutral (the pH of the washing water is about 7). Next, the precipitate is dried in the oven at a temperature of 110°C for 12 hours. The silica extraction precipitate is ground and sifted through a 325 mesh (45 μm) sieve. In this study, the method of extraction of silica with an acidic solution were used, so that the resulting silica was analyzed physical, chemical and thermal properties. Figure 1 shows the silica extraction process.

Sample characterization

In order to identify phase content, the Shimadzu XRD-D7000 machine was used, which was equipped with a Maxima X-Ray Diffractometer where X-rays are scanned continuously from an angle of 10 to 80 degrees 2-theta at a speed of 2.0 degrees per minute. The target X-ray tube is Cu with a voltage of 40.0 kV and a current of 30.0 mA. The two samples were crushed with pestle and mortar before being placed in a stainless-steel sample holder. MATCH! is used for data analysis (peak scanning and matching) – Phase Identification from Powder Diffraction Data - Version 2.4.7.

The surface functional groups of all samples were determined by Fourier-transform Infrared Spectroscopy using a SHIMADZU IR Prestige 21 apparatus. This was carried out between a wavelength of 400-4000 cm^{-1}, with a resolution of 41 cm^{-1} and 45 scanners. FTIR was able to accurately detect differences between compounds in coffee varieties (Amorocho-Cruz; Cortés, 2021). The surface topography, chemical composition and pore structure of the samples were analyzed using Scanning Electron Microscope with the JEOL-JSM-6510LV EDS detector.

To determine the surface area and pore structure of activated carbon samples, a nitrogen adsorption-desorption isotherm test was carried out at 77.3K using an automatic adsorption apparatus, Nova Quantachrome Instruments version 11.03 (Quantachrome Corporation, USA). Adsorption data were obtained at a relative pressure, P/Po, ranging from 0.01 to 0.1. Before testing, the sample was degassed inside a vacuum for 3 hours at a temperature of 300°C. Data calculation and analysis were carried out following the BET method. The TGA analyses were performed under the Termogravimetric analyzer Shimadzu DTG-60 with a high-temperature furnace by purging with nitrogen at a flow rate of 30 ml/min and heating

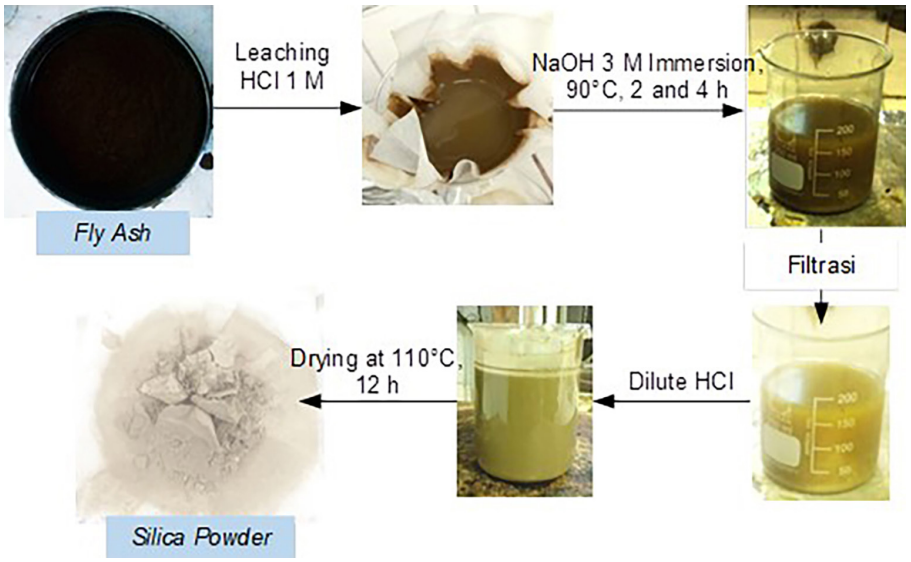

Figure 1. Silica extraction process

rate of 15 °C/min. The samples were placed in an alumina crucible c.a. 10 mg, then heated from an ambient temperature to 600 °C

RESULTS AND DISCUSSION

Phase content analysis

The XRD analysis results from samples (fly ash, silika_2, and silika_4) were obtained as shown in Figure 2 It is clearly visible that the peaks of the spectrum are very sharp related to the presence of crystal-structured phases that are characteristic of natural silica (Mourdikoudis et al., 2018). The presence of a sufficiently high crystalline phase in the fly ash of power plants indicates that not all minerals in the coal will melt completely during the combustion process. In addition, there are a number of inorganic materials that return in the form of fly ash crystals. On the other hand, after the coal is burned, there is a certain amount of material residue suspended in the smoke flow which can then reduce the temperature and the process of solidification occurs quickly to form a crystalline phase and an amorphous phase before finally being trapped in the electrostatic precipitator as fly ash.

The XRD spectrum of fly ash indicates a high content of silica in the form of quartz. Quartz is one of the very stable crystalline phases of silica other than cristobalite. The presence of metal alumina oxides associated with silica forms amorphous alumina-silicates. Alumina was also found as a separate particle with other elements in (2θ=37.6°) (Kim et al., 2012). In addition, there is a deep unburned carbon content (2θ=29.3°), as well as iron phase was found as hematide (2θ=35.3°). The high amount of silica, alumina, and iron content (more than 50%) indicates that fly ash from PLTU Aceh is classified as class C. This corresponds to the characteristics of medium-rank coal fly ash (sub bituminous) (Alterary and Marei, 2021). Although coal contains 10% lignite (low-rank coal), it does not affect the overall fly ash composition. Calcium is also related to alumina silicate which is characteristic of subbituminous coal fly ash (Strzałkowska, 2021).

The contact time between fly ash solids and NaOH extractant was varied, namely 2 hours and 4 hours. During this contact time, the silica in fly ash will dissolve in liquid NaOH form sodium silicate. The XRD data show that a contact time of 4 hours is capable of produces silica with a purity of up to 87%. This value is better than silica extraction samples with a contact time of 2 hours which resulted in 72% silica purity. In the two samples with different contact times, more than 75% of the material was found silica in the form of quartz. This comparison of XRD patterns shows that the peak intensity corresponding to the mullite phase has increased as a result of deep alumina enrichment in alkali leached fly ash residue. It can be attributed as has been explained by Tripathy, et. al., 2019, to the fact that the washing of fly ash with NaOH results in the dissolution of some silica, which in an amorphous state leaves the quartz phase intact (Tripathy et al., 2019). The peaks of the silica spectrum in the XRD pattern (Fig. 2) are summarized in Table 1.

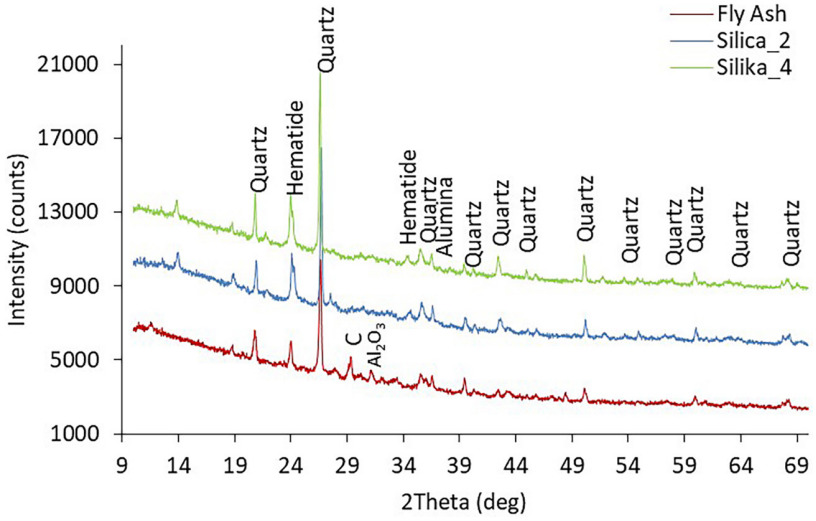

Figure 2. XRD pattern of the fly ash and silica extraction samples

Table 1. Silica spectrum from XRD pattern of fly ash (FA)

FA sample of the result		Literature		
2 θ (degree)	d (Å)	2θ(degree)	d (Å)	Reference
20.85 (quartz)	4.255	20.71	4.2896	(Wang et al., 2008)(Das et al., 2015)
26.61 (quartz)	3.346	26.61	3.3949	(Das et al., 2015)
36.51 (cristobalite)	2.458	36	-	(Besari et al., 2021) (Kordatos et al., 2008)
39.42	2.285	39.33		
40.22	2.239	40.23		
42.43	2.128	42.44		
44.96	2.014	45.99		
45.75	1.981	46.21	1.9648	(Das et al., 2015)
50.09 (quartz)	1.819	50.07	-	(Besari et al., 2021)
54.83	1.672	54.84		
68.11	1.375	68.12		

Even though the fly ash has already undergone acid washing using a solution HCl at the beginning of the silica extraction process but in the silica powder samples still found XRD spectrum peaks related to the presence of residual metal oxide impurities in the form of hematite, and alumina minerals although in low levels. A new phase also appears on XRD spectrum pattern of all silica powder ($2\theta=13.86^{o}$) which is characteristic of the zeolite phase (phillipsite) (Borodina et al., 2020). The appearance of the zeolite phase is due to the reaction between some silica and alumina with an alkaline solution during the silica extraction process. The variations that occurred at the peak intensity of all samples indicated that microstructure, chemical composition and impurity content in each sample there is little differences between each other. The purity of silica obtained through fly ash extraction is on average about 78.5%. This result is quite satisfactory when compared to an average of about 63% commercial silica purity in the presence of impurities in the form of iron oxides and alumina (Mariana et al., 2019).

BET analysis (Physisorption/adsorption-desorption isothermal N_2)

To determine the characteristics of the surface area and the nature of the porosity of fly ash, tested by nitrogen isothermal adsorption-desorption method or namely BET test. The results obtained are shown in Figure 2, the red line indicates the adsorption curve and the blue line for the desorption curve. Fly ash material originating from Aceh power plants according to the classification by IUPAC show physisorption properties Type IV isothermal is indicated by the formation of a hysteresis loop at a relative pressure of P/P_0 = 0.55–1.0. The hysteresis loop is a characteristic feature of the isothermal adsorption-desorption graph form by mesoporous material due to capillary condensation of nitrogen in the pores of the particles homogeneous particles. IUPAC distinguishes porous materials into three types, namely microporous (< 20 nm), mesoporous (20–500 nm) and macroporous (> 500 nm) (Ma et al., 2020).

Figure 3 shows that the amount of nitrogen absorbed by fly ash increases greatly after the relative pressure (P/Po) is greater than 0.5. On the basis of the BET method, the surface area of fly ash is 290 m^2/g, the pore volume is 0.4 cm^3/g, and the pore diameter is 23.3 nm (mesoporous). The pore size of fly ash which is larger than 0.7 nm shows an opportunity for its use as a hydrogen storage material. The calculations using the BET method correspond to the type of hysteresis loop for mesoporous materials.

Surface morphology and elemental analysis

The morphological results from SEM analysis in Figure 4 showed the microstructure of fly ash particles at 10,000× magnification. The morphological structure of fly ash contains organic and inorganic matter that forms a uniform plate agglomeration. The organic component is unburned carbon with a dark gray or black color with a fairly high spectrum intensity (21.09 wt%) in the EDS data and this explains the original fly ash color from the power plant in Aceh. The inorganic content is a crystalline phase mineral dominated by

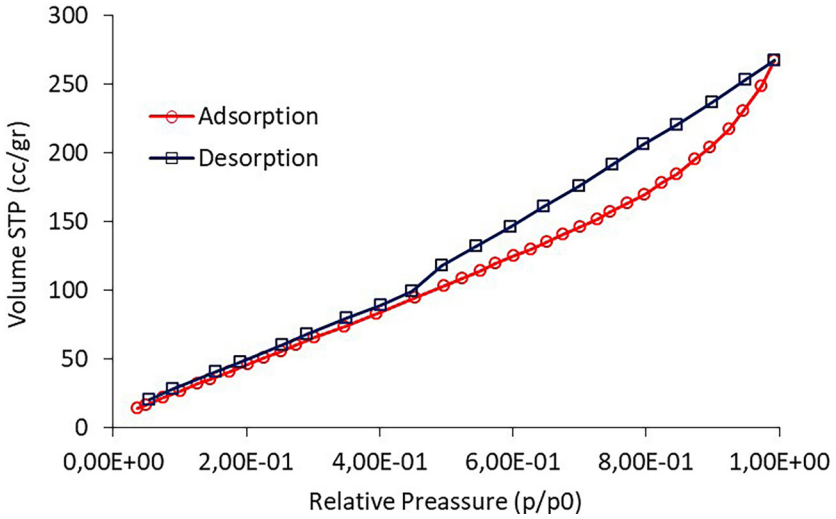

Figure 3. Adsorption-desorption isothermal N_2 of fly ash sample

silica in the form of quartz, alumina, and iron oxide followed by sodium. Quartz silica is identified angle-subrounded by white or clear color, as shown in the supplementary information of figure S1.

Table 1 shows the results of elemental analysis of EDS. The silica content of fly ash tends to increase after soaking with an acid solution for 1 hour 0.36%, while soaking for 4 hours with an acid solution increases by 4%. The high content of silica and alumina makes the fly ash of PLTU Aceh highly prospective to be used as raw material for zeolite synthesis (Vichaphund et al., 2014) and geopolymer synthesis (Eiamwijit et al., 2015). Zeolite is quite popular as a heterogeneous catalyst for biodiesel production while geopolymers are known as new materials to replace concrete. The intensity of the EDS spectrum is relatively weak for magnesium and calcium elements indicating a low concentration of these elements in the fly ash sample particles. Molybdenum, along with magnesium and calcium, is present as small elements forming the plural phase of fly ash compounds. It can be concluded that based on this analysis, in general the existing spectrum corresponds to chemical analysis.

FTIR analysis

Figure 5 shows the spectrum of the fly ash sample at the wavelength 400–4000 cm^{-1}. There are three vibration peaks related to the presence of silica, symmetric vibrations of the siloxanes (Si-O-Si) group at the wave number 470 cm^{-1} (Yan F. et al., 2017), symmetric vibrations of Al–O and Si-O at wave numbers 785 cm^{-1} relating to quartz silica and vibration of the functional groups Si-O=Si and Si-O-Al at wave number 1008 cm^{-1} which is trydimite silica. Generally, the vibrations at the wavenumber region of 1000-1020 cm^{-1} describe the bonds of the Si-O=Si and Al-O-Si functional groups typical for the presence of silica (Rondon W, et al. 2013). The silica functional group in fly ash also indicates the presence of silicon atoms associated with aluminum atoms forming aluminum-silicate. The presence of carbonate ions (calcite) is indicated by the vibration of C-O at wave number 1477 cm^{-1} and the presence of organic matter from the carboxylate group C=O is characterized by vibration at wave number 1627 cm^{-1} (Jeyageetha CJ and Kumar SP, 2013).

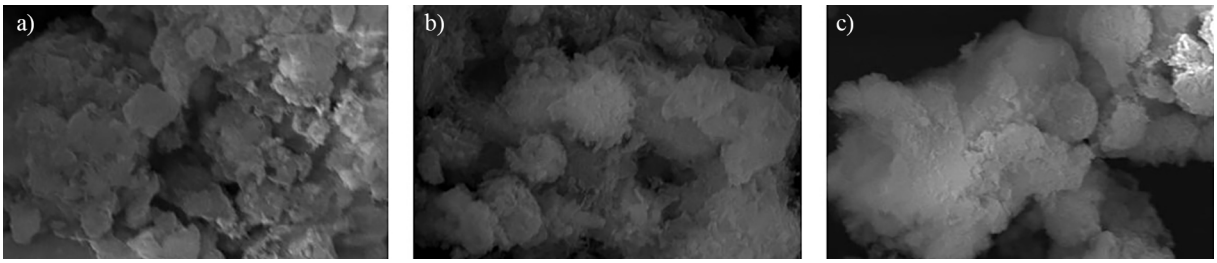

Figure 4. Scanning electron micrograph of (a) fly ash, (b) silika_2 and (c) silika_4

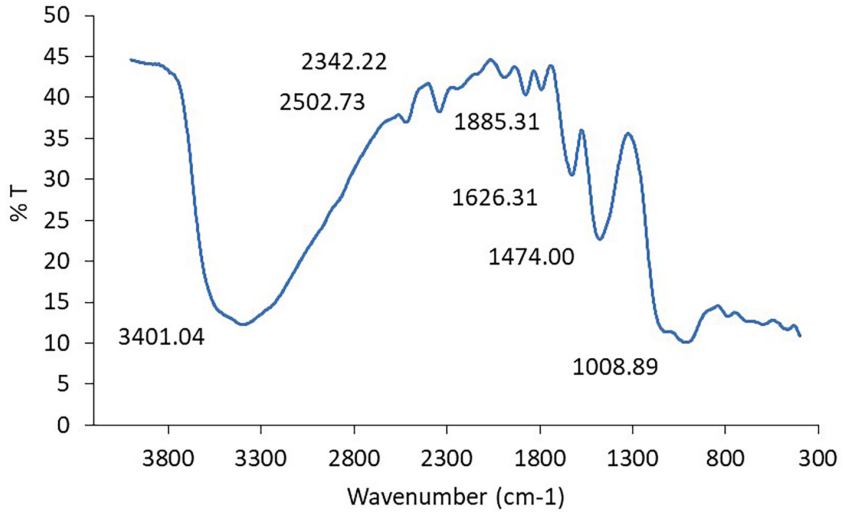

Fig. 5. FTIR spectrum of fly ash sample

Figure 6 is the FTIR spectrum of extracted silica samples under different conditions. The spectrum produces several peaks indicating the presence of several functional groups such as silica or functional groups from impurities that cannot be completely cleaned. The spectra of all samples showed very similar position and intensity of the absorption bands indicating the presence of the same functional group in all samples. This corresponds to the results of phase tests with XRD spectra showing almost similar patterns for all samples. In all silica samples, the main band with the greatest intensity was found to be within the region of wave numbers 1000–1020 cm^{-1} which indicates the presence of vibrations of the Si-O=Si and Si-O-Al silica groups (Pieter A. et al., 2012; Rondon W. et al., 2013).

Although the FTIR spectrum pattern for Silika_2 sample is similar to Silika_4, a slight difference was found, namely the presence of Si-O siloxane bending vibration at a wave number of about 2364 cm^{-1} in the Silika_4 sample which indicates silica phase (Besari D.A.A., et al., 2021) that contributes to the increased purity of the sample Silika_4 as indicated by the XRD spectrum pattern. The increase in extraction time from 2 hours to 4 hours also affects the value of the wave number on the FTIR spectrum. The wave number of silica samples with a 4-hour extraction time (Silica_4) treatment is enlarged compared to silica samples with an extraction time of 2 hours (Silica_2). The magnification of the wave number value is related to the increase in energy on the material surface (surface free energy) as a result

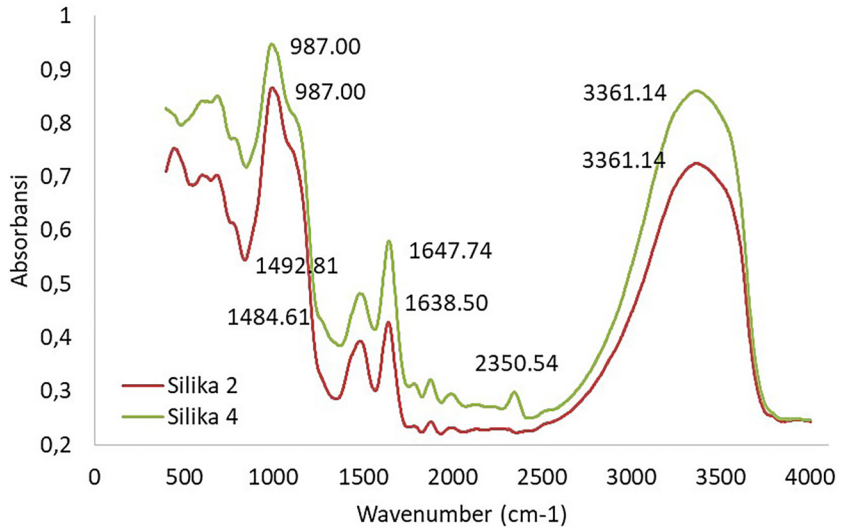

Fig. 6. FTIR spectrum of silica sample

of a decrease in the bond length between atoms/molecules of the functional group contained on the surface of silica powder. Furthermore, the rise in surface energy will contribute to an improvement in the surface mechanical properties of silica particles that are so necessary for heterogeneous catalyst applications (Yuksel, I. 2018).

Thermal analysis

To determine the thermal properties of fly ash and silica powder samples, extracted from fly ash, then a thermal analysis was carried out using analysis thermogravimetry (TGA) and differential scanning calorimetry (DSC). Figure 7 is TGA curve and Figure 8 is the DSC curve. The TGA curve shows a reduction in the mass of fly ash when heated from room temperature to 600°C. At temperatures of 59°C to 160°C, a total mass loss of about 15.5% occurs. This mass reduction is related to the moisture content and residual substances of volatile materials contained in fly ash. After passing through these temperatures the mass of fly ash tends to be constant. Generally, a drastic decrease at 200°C is strongly associated with water molecules adsorbed on the fly ash surface and structurally bound water within the nano silica framework as silanol which is slowly released from the fly ash surface with increasing heating temperature (Yan et al., 2017). Nano-silica refers to the particles with size of < 100 nm (Khairan et al., 2019; Jalil et al., 2018). In the fly ash DSC curve, there are two of endothermic reactions that occur associated with mass loss indicated by the peak of the curve leading to lower. The curve peak for the endothermic reaction I occurs at a temperature of about 112.9°C and peak endothermic reaction II occurs at a temperature of about 157°C. There is an endothermic reaction III which peaks at a temperature of 440°C and does

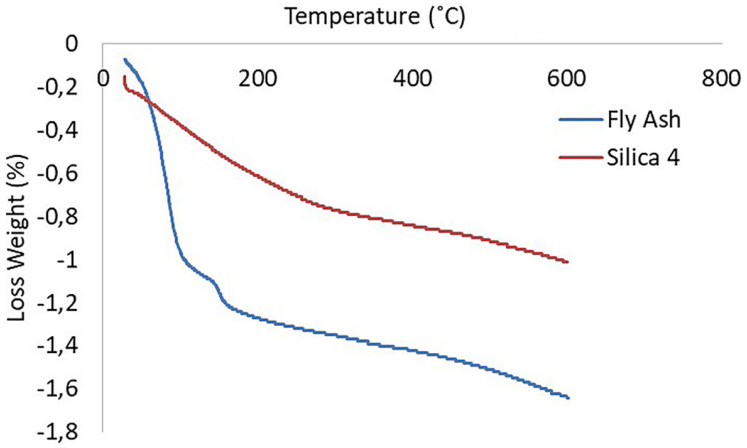

Fig. 7. TGA curve of fly ash and silica samples

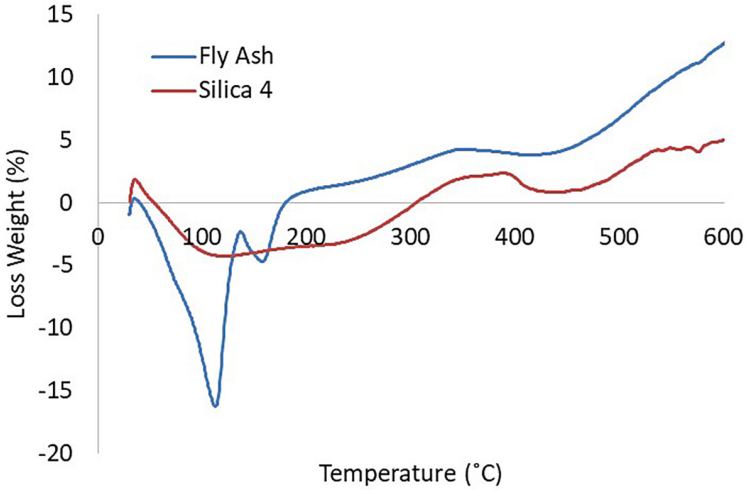

Fig. 8. DSC curve of fly ash and silica samples

not involve a decrease in the mass of fly ash at TGA curve. An endothermic reaction that occurs when there is no reduction in the mass of the ash particles flying is thought to be the area where the non-silicate phase transformation occurs or the formation of polymorphs of non-silicate compounds (Rondón W. et al., 2013).

The TGA curve for silica powder samples showed an 8% mass reduction at 44°C temperature of 119°C correlated with the endothermic reaction I on the DSC curve. This event is also related to the loss of adsorbed water molecules on the silica surface and the gradual release of water molecules in the silanol group into a siloxane group. After a temperature of 120°C the silica mass tends to be constant because all silanol groups have been condensed into siloxane (Bera and Das, 2019). Overall, the silica sample shows a fairly good thermal stability, especially in the temperature range between 120°C and 300°C. Thermal stability is important characteristics of catalyst materials required for optimization of internal diffusion during reaction (Monfort et al., 2014).

CONCLUSIONS

It has been successfully extracted silica from fly ash using alkaline solution sodium hydroxide catalyzed by a hydrochloric acid solution. Fly ash as raw the material shows the character of a mesoporous material with a nitrogen adsorption-desorption curve in the form of an isothermal type IV H3 mode with a specific surface area reaching 290 m^2/gr and the pore size at the surface is about 23.3 nm making it suitable for use as a hydrogen storage material. The FTIR spectrum data shows the content of the silanol group and siloxane which forms crystalline silica of the types of quartz, cristobalite and tridymite. On the basis of the XRD and EDS data, the fly ash of the Aceh power plant belongs to the class C with a high content of crystalline silica and alumina so that it has the potential as a raw material for the synthesis of zeolite and geopolymer. On the basis of the TGA/DSC data for silica which extracted from fly ash showed quite good thermal stability with the morphology of the structure consists of an arrangement of grains such as uniform plates that are agglomerated in size less than 1 micron as shown by SEM data. The FTIR silica data shows that the reaction time increases from 2 hours to 4 hours has shifted the wavenumber associated with decreasing bond length between atoms of the functional groups as an indication of the improvement of the mechanical properties of silica particles. The reaction time is 4 hours between fly ash as reactant and NaOH as reactant produces silica as an extractant with a purity of up to 87%, higher compared to the reaction time of only 2 hours which produces silica with a purity of 72%. In general, the characteristics of silica that have been obtained in this study can be used as an initial reference on the production of crystalline silica powder made from fly ash waste for industrial scale and wider applications. Furthermore, the characteristics of silica are potential as a heterogeneous catalyst material can still be improved by further studies pertaining to optimization of synthesis parameters in the form of reactant concentrations, initial purity of raw materials (fly ash), acid solution concentration, thermal conditions, and reaction time.

Acknowledgments

The authors acknowledge the Directorate of Research, Technology, and Community Service, Ministry of Education, Culture, Research and Technology, Republic of Indonesia for their sponsorship under doctoral dissertation research scheme, contract number: 581/UN11.2.1/ PT.01.03/ DRPM/2023.

REFERENCES

1. Abu Bakar, A.H., Jia Ni Carey, C. 2020. Extraction of Silica from Rice Straw Using Alkaline Hydrolysis Pretreatment. IOP Conf. Ser. Mater. Sci. Eng., 778. https://doi.org/10.1088/1757-899X/778/1/012158
2. Alterary, S.S., Marei, N.H. 2021. Fly ash properties, characterization, and applications: A review. J. King Saud Univ. - Sci., 33, 101536. https://doi.org/10.1016/j.jksus.2021.101536
3. Anas Boussaa, S., Kheloufi, A., Boutarek Zaourar, N., Bouachma, S. 2017. Iron and aluminium removal from Algerian silica sand by acid leaching. Acta Phys. Pol. A, 132, 1082–1086. https://doi.org/10.12693/APhysPolA.132.1082
4. Bera, B., Das, N. 2019. Synthesis of high surface area mesoporous silica SBA-15 for hydrogen storage application. Int. J. Appl. Ceram. Technol., 16, 294–303. https://doi.org/10.1111/ijac.13082
5. Besari, D.A.A., Anggara, F., Petrus, H.T.B.M., Astuti, W., Husnah, W.A. 2021. Effect of power plant operating conditions on fly ash and bottom

ash composition: A case study from power plant in Lampung. IOP Conf. Ser. Earth Environ. Sci., 851. https://doi.org/10.1088/1755-1315/851/1/012039

6. Bhatt, A., Priyadarshini, S., Acharath Mohanakrishnan, A., Abri, A., Sattler, M., Techapaphawit, S. 2019. Physical, chemical, and geotechnical properties of coal fly ash: A global review. Case Stud. Constr. Mater., 11, e00263. https://doi.org/10.1016/j.cscm.2019.e00263
7. Blissett, R. 2015. Coal fly ash and the circular economy, 1–248.
8. Borodina, U., Goryainov, S., Oreshonkov, A., Shatskiy, A., Rashchenko, S. 2020. Raman study of 3.65 Å-phase MgSi(OH)6 under high pressure and the bands assignment. High Pressure Research, 40(4), 495–510. https://doi.org/10.1080/08957959.2020.1830078
9. Das, D., Samal, D.P., BC, M. 2015. Preparation of Activated Carbon from Green Coconut Shell and its Characterization. J. Chem. Eng. Process Technol., 06. https://doi.org/10.4172/2157-7048.1000248
10. Dhaneswara, D., Fatriansyah, J.F., Situmorang, F.W., Haqoh, A.N. 2020. Synthesis of Amorphous Silica from Rice Husk Ash: Comparing HCl and CH3COOH Acidification Methods and Various Alkaline Concentrations. Int. J. Technol., 11, 200–208. https://doi.org/10.14716/ijtech.v11i1.3335
11. Eiamwijit, M., Pachana, K., Kaewpirom, S., Rattanasak, U., Chindaprasirt, P. 2015. Comparative study on morphology of ground sub-bituminus FBC fly ash geopolymeric material. Adv. Powder Technol., 26, 1053–1057. https://doi.org/10.1016/j.apt.2015.04.013
12. Fomenko, E. V., Anshits, N.N., Solovyov, L.A., Knyazev, Y. V., Semenov, S. V., Bayukov, O.A., Anshits, A.G. 2021. Magnetic Fractions of PM2.5, PM2.5-10, and PM10from Coal Fly Ash as Environmental Pollutants. ACS Omega 6, 20076–20085. https://doi.org/10.1021/acsomega.1c03187
13. Foo, C.T., Salleh, M.A.M., Ying, K.K., Matori, K.A. 2019. Mineralogy and thermal expansion study of mullite-based ceramics synthesized from coal fly ash and aluminum dross industrial wastes. Ceram. Int., 45, 7488–7494. https://doi.org/10.1016/j.ceramint.2019.01.041
14. Gruchot, A., Zydroń, T. 2016. Impact of a test method on the undrained shear strength of a chosen fly ash. J. Ecol. Eng., 17, 41–49. https://doi.org/10.12911/22998993/63955
15. Guo, C., Zou, J., Ma, S., Yang, J., Wang, K. 2019. Alumina extraction from coal fly ash via low-temperature potassium bisulfate calcination. Minerals, 9. https://doi.org/10.3390/min9100585
16. Handoko, E., Budi, E., Sugihartono, I., Marpaung, M.A., Jalil, Z., Taufiq, A., Alaydrus, M. 2020. Microwave absorption performance of barium hexaferrite multi-nanolayers, Mater. Express, 10 (8), 1328–1336. DOI: 10.1166/mex.2020.1811
17. Jalil, Z., Rahwanto, A., Malahayati, Mursal, Handoko, E., Akhyar, H. 2018. Hydrogen storage properties of mechanical milled MgH_2-nano Ni for solid hydrogen storage material, IOP Conf. Ser.: Mater. Sci. Eng., 432, 012034. DOI: 10.1088/1757-899X/432/1/012034
18. Jeyageetha C.J., Kumar S.P. 2013. Study of SEM/EDXS and FTIR for Fly Ash to Determine the Chemical Changes of Ash in Marine Environment. Int J Sci Res., 5(7), 2319–7064.
19. Juda-Rezler, K., Kowalczyk, D. 2013. Size distribution and trace elements contents of coal fly ash from pulverized boilers. Polish J. Environ. Stud., 22, 25–40.
20. Kim, H.S., Park, N.K., Lee, T.J., Um, M.H., Kang, M. 2012. Preparation of nanosized α - Al_2O_3 particles using a microwave pretreatment at mild temperature. Adv. Mater. Sci. Eng., 2012. https://doi.org/10.1155/2012/920105
21. Kordatos, K., Gavela, S., Ntziouni, A., Pistiolas, K.N., Kyritsi, A., Kasselouri-Rigopoulou, V. 2008. Synthesis of highly siliceous ZSM-5 zeolite using silica from rice husk ash. Microporous Mesoporous Mater., 115, 189–196. https://doi.org/10.1016/j.micromeso.2007.12.032
22. Khairan, K., Zahraturriaz, Z., Jalil, Z. 2019. Green synthesis of sulphur nanoparticles using aqueous garlic extract (allium sativum). Rasayan Journal of Chemistry, 12(1) 50–57. http://dx.doi.org/10.31788/RJC.2019.1214073
23. Lindvall, M., Berg, M., Sichen, D. 2017. The Effect of Al2O3, CaO and SiO2 on the Phase Relationship in FeO–SiO2 Based Slag with 20 Mass% Vanadium. J. Sustain. Metall., 3, 289–299. https://doi.org/10.1007/s40831-016-0088-y
24. Ma, Z., Gao, J., Weng, X., Yang, S., Peng, K. 2020. Synthesis and mechanism of aluminum silicate mesoporous materials by F108 template. Mater. Sci. Pol., 38, 566–576. https://doi.org/10.2478/msp-2020-0067
25. Mariana, M., Mulana, F., Sofyana, S., Dian, N.P., Lubis, M.R. 2019. Characterization of adsorbent derived from Coconut Husk and Silica (SiO2). IOP Conf. Ser. Mater. Sci. Eng., 523. https://doi.org/10.1088/1757-899X/523/1/012022
26. Mirda, E., Idroes, R., Khairan, K., Tallei, T.E., Ramli, M., Earlia, N., Maulana, A., Idroes, G. M., Muslem, M., Jalil, Z. 2021. Synthesis of Chitosan-Silver Nanoparticle Composite Spheres and Their Antimicrobial Activities, Polymers, 13(22), 3990. https://www.mdpi.com/2073-4360/13/22/3990
27. Mohammed Hello, K., Kadhim Hlial, E. 2019. Modification of silica with sulfuric acid and phosphoric acid for cellulose hydrolysis. J. Phys. Conf. Ser., 1294. https://doi.org/10.1088/1742-6596/1294/5/052013
28. Monfort, E., Mezquita, A., Vaquer, E., Celades,

I., Sanfelix, V., Escrig, A. 2014. Ceramic Manufacturing Processes: Energy, Environmental, and Occupational Health Issues, Comprehensive Materials Processing, Elsevier. https://doi.org/10.1016/B978-0-08-096532-1.00809-8

29. Mourdikoudis, S., Pallares, R.M., Thanh, N.T.K. 2018. Characterization techniques for nanoparticles: Comparison and complementarity upon studying nanoparticle properties. Nanoscale, 10, 12871–12934. https://doi.org/10.1039/c8nr02278j
30. Muthusamy, K., Rasid, M.H., Jokhio, G.A., Mokhtar Albshir Budiea, A., Hussin, M.W., Mirza, J. 2020. Coal bottom ash as sand replacement in concrete: A review. Constr. Build. Mater., 236, 117507. https://doi.org/10.1016/j.conbuildmat.2019.117507
31. Petrus, H.T.B.M., Olvianas, M., Suprapta, W., Setiawan, F.A., Prasetya, A., Sutijan, A.F. 2020. Cenospheres Characterization from Indonesian Coal-Fired Power Plant Fly Ash and Their Potential Utilization. Journal of Environmental Chemical Engineering, 8, 104116. https://doi.org/10.1016/j.jece.2020.104116
32. Pieter A., Cozmuta L.M., Cozmuta A.M., Nicula C., Indrea E., Tutu H. 2012. Calcium- and ammonium ion-modification of zeolite amendments affects the metal- uptake of Hieracium piloselloides in a dose-dependent way. J Environ Monit.,; 14, 2807e14.
33. Rondón, W., Freire, D., Benzo, Z. de, Sifontes, A.B., González, Y., Valero, M., Brito, J.L. 2013. Application of 3A Zeolite Prepared from Venezuelan Kaolin for Removal of Pb (II) from Wastewater and Its Determination by Flame Atomic Absorption Spectrometry. Am. J. Anal. Chem., 4, 584–593. https://doi.org/10.4236/ajac.2013.410069
34. Sefriani, R., Oktavia, B. 2021. Modification of natural silica using dimethylamine and the application as a phosphate ion absorption. J. Phys. Conf. Ser., 1788. https://doi.org/10.1088/1742-6596/1788/1/012015
35. Song, H., Tang, M., Lei, X., Feng, Z., Cheng, F. 2020. Preparation of ultrafine fly ash-based superhydrophobic composite coating and its application to foam concrete. Polymers (Basel)., 12. https://doi.org/10.3390/POLYM12102187
36. Strzałkowska, E. 2021. Morphology and chemical composition of mineral matter present in fly ashes of bituminous coal and lignite. Int. J. Environ. Sci. Technol., 18, 2533–2544. https://doi.org/10.1007/s13762-020-03016-0
37. Tripathy, A.K., Behera, B., Aishvarya, V., Sheik, A.R., Dash, B., Sarangi, C.K., Tripathy, B.C., Sanjay, K., Bhattacharya, I.N. 2019. Sodium fluoride assisted acid leaching of coal fly ash for the extraction of alumina. Miner. Eng., 131, 140–145. https://doi.org/10.1016/j.mineng.2018.10.019
38. Vichaphund, S., Aht-Ong, D., Sricharoenchaikul, V., Atong, D. 2014. Characteristic of fly ash derived-zeolite and its catalytic performance for fast pyrolysis of Jatropha waste. Environ. Technol. (United Kingdom), 35, 2254–2261. https://doi.org/10.1080/09593330.2014.900118
39. Vielma, T., Lassi, U., Salminen, J. 2018. Precipitation of silica from zinc process solution. Monatshefte fur Chemie, 149, 313–321. https://doi.org/10.1007/s00706-017-2054-1
40. Vilakazi, A.Q., Ndlovu, S., Chipise, L., Shemi, A. 2022. The Recycling of Coal Fly Ash: A Review on Sustainable Developments and Economic Considerations. Sustain., 14, 1–32. https://doi.org/10.3390/su14041958
41. Wang, S., Ma, Q., Zhu, Z.H. 2008. Characteristics of coal fly ash and adsorption application. Fuel, 87, 3469–3473. https://doi.org/10.1016/j.fuel.2008.05.022
42. Wang, Z., Dai, S., Zou, J., French, D., Graham, I.T. 2019. Rare earth elements and yttrium in coal ash from the Luzhou power plant in Sichuan, Southwest China: Concentration, characterization and optimized extraction. Int. J. Coal Geol., 203, 1–14. https://doi.org/10.1016/j.coal.2019.01.001
43. Yadav, V.K., Fulekar, M.H. 2020. Advances in methods for recovery of ferrous, alumina, and silica nanoparticles from fly ashwaste. Ceramics, 3, 384–420. https://doi.org/10.3390/ceramics3030034
44. Yan, F., Jiang, J., Li, K., Liu, N., Chen, X., Gao, Y., Tian, S. 2017. Green Synthesis of Nanosilica from Coal Fly Ash and Its Stabilizing Effect on CaO Sorbents for CO2 Capture. Environ. Sci. Technol., 51, 7606–7615. https://doi.org/10.1021/acs.est.7b00320
45. Yao, Z.T., Ji, X.S., Sarker, P.K., Tang, J.H., Ge, L.Q., Xia, M.S., Xi, Y.Q. 2015. A comprehensive review on the applications of coal fly ash. Earth-Science Rev., 141, 105–121. https://doi.org/10.1016/j.earscirev.2014.11.016
46. Yuksel I. Blast-furnace slag. 2018. Waste and Supplementary Cementitious Materials in Concrete: Characterisation, Properties and Applications. Elsevier Ltd., 361–415. http://dx.doi.org/10.1016/B978-0-08-102156-9.00012-2